

P12.160 THE TORNADOGENESIS PHASE OF A VORTEX2 SUPERCELL TORNADO ON JUNE 7, 2010

Elizabeth A. Davidson* and Donald W. Burgess
The University of Oklahoma, Cooperative Institute for Mesoscale Meteorological Studies,
and NOAA, NSSL, Norman, OK

1. INTRODUCTION

The NOAA (NSSL) X-band dual-Polarized (NOXP) and three CSWR Doppler on Wheels (DOW5, DOW6, and DOW7) mobile radars scanned the second of two supercells on 7 June 2010 (see Figure 1 for locations). The two supercells on this day occurred during the Verification of the Origins of Rotation in Tornadoes Experiment, Part 2 (VORTEX2) field project (for more background information see Wurman et al. 2012). NOXP first deployed near Lyman, NE at about 2330 Z and collected data on a supercell that produced a tornado north of Scottsbluff, NE. This first supercell weakened and moved too far east to sample, and a second supercell, behind the first, was targeted (Figure 2). NOXP deployed just west of Minatare and collected data on the second supercell from 0112 Z to 0128 Z at the NOXP1 location, as indicated in Figure 1. DOW6 deployed and collected data from 0104 Z to 0118 Z at the DOW6 location marked on Figure 1. This is the only DOW data that has been analyzed thus far. Dual-Doppler analysis of the DOW6 and NOXP 0116-0118 Z volume scan is used to investigate the genesis of a weak (EF1), but rather long-lasting (19 mile length) tornado, that touched down at about 0121 Z.

2. METHODOLOGY AND DATA PREPARATION

2.1 Data Collection

The VORTEX2 field campaign spanned eleven and ½ weeks during the spring of 2009 and 2010. NOXP operated as a dual-polarization mesocyclone-scale radar in VORTEX2, along with DOW6 and DOW7, to provide low- to mid-level coverage of the right flanks of supercells being targeted by armada sensors. These radars typically scan a storm from about 5-30 km distance. The mesocyclone-scale radar observations, along with storm- and tornado-scale observations, allow for dual-Doppler synthesis to reconstruct important kinematic fields, such as vorticity and divergence, within and around the storm. DOW5 is a rapid-scan radar, which was operated as a tornado-scale radar in VORTEX2. In 2010, DOW6 and DOW7 were upgraded to dual-frequency, dual-polarization capability. This and other similarities in their operating characteristics facilitated dual-Doppler analyses with NOXP. NOXP and DOW6 configuration parameters for spring 2010 are shown in Table 1.

*Corresponding author address: Elizabeth A. Davidson, University of Oklahoma, School of Meteorology, 120 David L. Boren Blvd., Rm 3920A, Norman, OK 73072-7307; email: erockwell@ou.edu

Table 1 – Specifications for the NOXP and DOW6 mobile weather radars during VORTEX2 Spring 2010.

Name	NOXP	DOW6
Wavelength	3 cm	2 x 3cm
Frequency	9.41 GHz	9.40 GHz, 9.55GHz
3-dB Beamwidth	0.95°	0.93°
Antenna Rotation Rate	29°/s	50°/s
Peak Power	250kW	2 x 250kW
PRF	2500 Hz	Up to 5000 Hz (staggered)
Nyquist Interval	+/- 19.9 m/s	+/- 78 m/s
Gate Spacing	75m	30-60m
Polarization	dual	dual
Volume Time	2 min	2 min
Scanning Strategy	1°-7° (1° interval), 360° full scans	0.5°, 1°-6°, 0.5°, 1°, 8°-14° (2° intervals), 360° full scans

2.2 Data Preparation

NOXP and DOW6 data were de-cluttered and de-aliased (NOXP only) using Solo II (Oye et al. 1995). Heading corrections had already been performed by the scientists that collected the data. The edited sweep files were converted to NetCDF format using the Foray translator developed by Dennis Flannigan at the National Center for Atmospheric Research (NCAR).

Attenuation and differential attenuation limit observations of reflectivity and differential reflectivity signatures at X-band. As hydrometeor diameters become closer in size to the radar wavelength, attenuation becomes more prevalent. Attenuation is effected by the hydrometeor type, concentration, and distribution within the resolution volume. The ZPHI Rain-Profiling algorithm and the Gamma technique (Snyder 2008) are applied to mitigate attenuation and differential attenuation in an attempt to correct the NOXP data and better identify signatures in supercell thunderstorms.

The data from both NOXP and DOW6 were also smoothed through an objective analysis. A 3-Dimensional Barnes 2-pass objective analysis scheme (Barnes 1964; Koch et al. 1983; Majcen et al. 2008) was applied to each field acquired by the radar. The Barnes (1973) objective analysis scheme uses a Gaussian weighted-averaging technique, which assigns a weight to a datum solely as a known function of distance between the datum and grid point (Koch et al. 1983). The convergence parameter γ is chosen to be a constant value of 0.3 following the experiments in Majcen et al. (2008) and the recommendation from Barnes (1973) that this parameter is best chosen from the range 0.2 to 0.4. The smoothing parameter κ_0 varies

based on the proximity of the echo to the radar (Pauley and Wu 1990). Approximate storm propagation was accounted for in the objective analysis. This objective analysis interpolates data from polar coordinates to a Cartesian grid for use in dual-Doppler syntheses. The objectively analyzed data can also be plotted as a Constant Altitude Plan Position Indicator (CAPPI) using a MATLAB program. The 4/3 Earth's radius rule found in Doviak and Zrnic (1993) is used to plot each field at a constant altitude.

The dual-Doppler wind synthesis software package, developed by Conrad Ziegler (Ziegler 1978), uses two objective analysis output files to reconstruct the three-dimensional wind field. The output of the dual-Doppler synthesis is viewed using MATLAB scripts that overlay smoothed dual-polarimetric fields and the extracted Cartesian wind components.

3. DATA ANALYSIS AND RESULTS

Dual-Doppler analysis was performed on the 0116 – 0118 Z volume scan. The attenuation corrected, objectively analyzed NOXP dual-polarimetric fields were overlaid with the calculated wind vectors. The radial velocity data from both radars were used to calculate wind vectors within the dual-Doppler lobe, in which the angle between the two radar beams was greater than 28° and less than 150° . Due to the close proximity of both radars to the storm at this time (less than 20 km), data above about 2.5 km were not retrievable due to the cone of silence extending into the radar echoes from the storm. A portion of the storm's right flank and weak echo region (WER) lie along the dual-Doppler baseline, a region where wind synthesis is not possible. Lower level (600m) and higher level (1800m) dual-Doppler syntheses were selected for comparison, as shown in Figures 3 and 4.

Strong inflow winds and convergence in the wind vectors at 600m (Figure 3) indicate the location of the updraft. The positive vertical velocity at 600m (Figure 4) is collocated with the area of convergence at 600m, supporting this location of the updraft. Similarly, there are indications of the updraft in the reflectivity, differential reflectivity and correlation coefficient fields.

Some weak rotation can be detected in the converging winds near the updraft at 600m. This area of strong low-level convergence with weak rotation at 600m is beneath an area of strong rotation at 1800m. The rotation in the updraft aloft is detected in the high, positive values of vertical vorticity at 1800m (Figure 4).

Hail signatures, collocated at both heights (Figure 3), are indicated by high reflectivity, low differential reflectivity, and low correlation coefficient. A smaller-area hail signature is located near $X=23$, $Y=18$, and a larger-area hail signature is centered near $X=25$, $Y=23$. Both hail areas are within the downdraft that flanks the main updraft on the north and west. There is some evidence of a Zdr arc, as noted by the high differential reflectivity (Zdr) values along the forward flank reflectivity gradient. A Zdr arc is indicative of size sorting of hydrometeors by the Storm Relative Environmental Helicity (SREH) (Kumjian and Ryzhkov 2008, 2009).

The 1800m wind fields show very low wind speeds in the rear flank region of the storm, and very little negative vertical velocity (downdraft), contrary to what might be expected in the rear flank downdraft region of a supercell.

4. CONCLUSIONS AND FUTURE WORK

The volume scan used for this dual-Doppler analysis is approximately 5 minutes prior to tornadogenesis, showing strong rotation aloft, but only weak rotation at lower levels. Very rapid evolution was documented over the next few minutes as a low-level rotation signature, strong rearflank downdraft winds, and a wrapping hook echo all developed, as shown in Figure 5. Therefore, some process must be acting quickly to initiate strong rotation at low levels prior to tornadogenesis. A hail signature is noted in close proximity to the rotating updraft, suggesting microphysical changes could play a role in the processes leading to tornadogenesis. The lack of a significant rear flank downdraft (RFD) approximately 5 minutes before tornadogenesis is unusual and needs further investigation. Future work includes using DOW5 and DOW7 data for additional dual-Doppler analyses, as DOW6 ended data collection after the volume scan used in this paper.

5. ACKNOWLEDGEMENTS

We would like to thank Chris Schwarz for all of his help with NOXP data preparation. We would also like to thank Conrad Ziegler and David Dowell for their help with the objective analysis program. We thank Nolan Atkins and his team for the damage survey information. Funding for this study comes from the NSF Grant ATM-0802717 and NOAA-University of Oklahoma Cooperative Agreement #NA11OAR430072.

6. REFERENCES

- Barnes, S. L., 1964: A Technique for Maximizing Details in Numerical Weather Map Analysis. *J. Appl. Meteor.*, **3**, 396–409.
- Barnes, S. L., 1973: Mesoscale objective analysis using weighted time-series observations. NOAA Tech. Memo. ERL NSSL-62, National Severe Storms Laboratory, Norman, OK 73069, 60pp [NTIS COM-73-10781]
- Doviak, R. J., and D. S. Zrnic, 1993: *Doppler Radar and Weather Observations*. Academic Press, 562 pp.
- Koch, S. E., M. desJardins, P. J. Kocin, 1983: An Interactive Barnes Objective Map Analysis Scheme for Use with Satellite and Conventional Data. *J. Climate Appl. Meteor.*, **22**, 1487–1503.
- Kumjian, M.R., and A. V. Ryzhkov, 2008: Polarimetric signatures in supercell thunderstorms. *J. Appl. Meteor. and Climatology*, **48**, 1940-1961.
- Kumjian, M.R., and A. V. Ryzhkov, 2009: Storm relative helicity revealed from polarimetric radar measurements. *J. Atmos. Sci.*, **66**, 667-685.

Majcen, M., P. Markowski, Y. Richardson, D. Dowell, and J. Wurman, 2008: Multipass Objective Analyses of Doppler Radar Data. *J. Atmos. Oceanic Technol.*, **25**, 1845–1858.

Oye, R., C.K.Mueller, and S. Smith, 1995: Software for radar translation, visualization, editing, and interpolation. Preprints, *27th Conference on Radar Meteorology*, Vail, CO, American Meteorological Society, 359-361.

Pauley, P. M., and X. Wu, 1990: The Theoretical, Discrete, and Actual Response of the Barnes Objective Analysis Scheme for One- and Two-Dimensional Fields. *Mon. Wea. Rev.*, **118**, 1145–1164.

Wurman, Joshua, David Dowell, Yvette Richardson, Paul Markowski, Erik Rasmussen, Donald Burgess, Louis Wicker, Howard B. Bluestein, 2012: The Second Verification of the Origins of Rotation in Tornadoes Experiment: VORTEX2. *Bull. Amer. Meteor. Soc.*, **93**, 1147–1170.

Ziegler, C. L., 1978: A dual-Doppler variational objective analysis as applied to the studies of convective storms. M.S. Thesis, University of Oklahoma, 115 pp. [Available from School of Meteorology, University of Oklahoma, 120 David L. Boren Blvd., Norman, OK 73072



Figure 1. Damage survey of wind (blue outline) and tornado (white circles and red outline) for June 7, 2010. Lighter shading is concentrated area of EF0 damage, darker shading is EF1 damage. NOXP1 is location of data collection; NOXP2 is location of tornado observation. DOW5, DOW6, and DOW7 locations also shown.

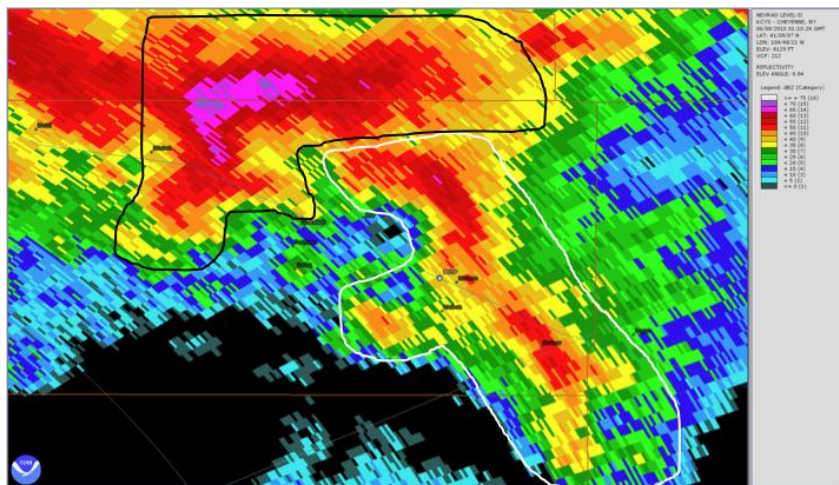


Figure 2. Reflectivity (0.5°) from KCYS at 0110 UTC on June 8 (evening of June 7), 2010. Dark outline is target storm. White outline is left-moving, short line segment that passed ahead of target storm. Location of NOXP marked. Image from NCDC Level2 Data Viewer.

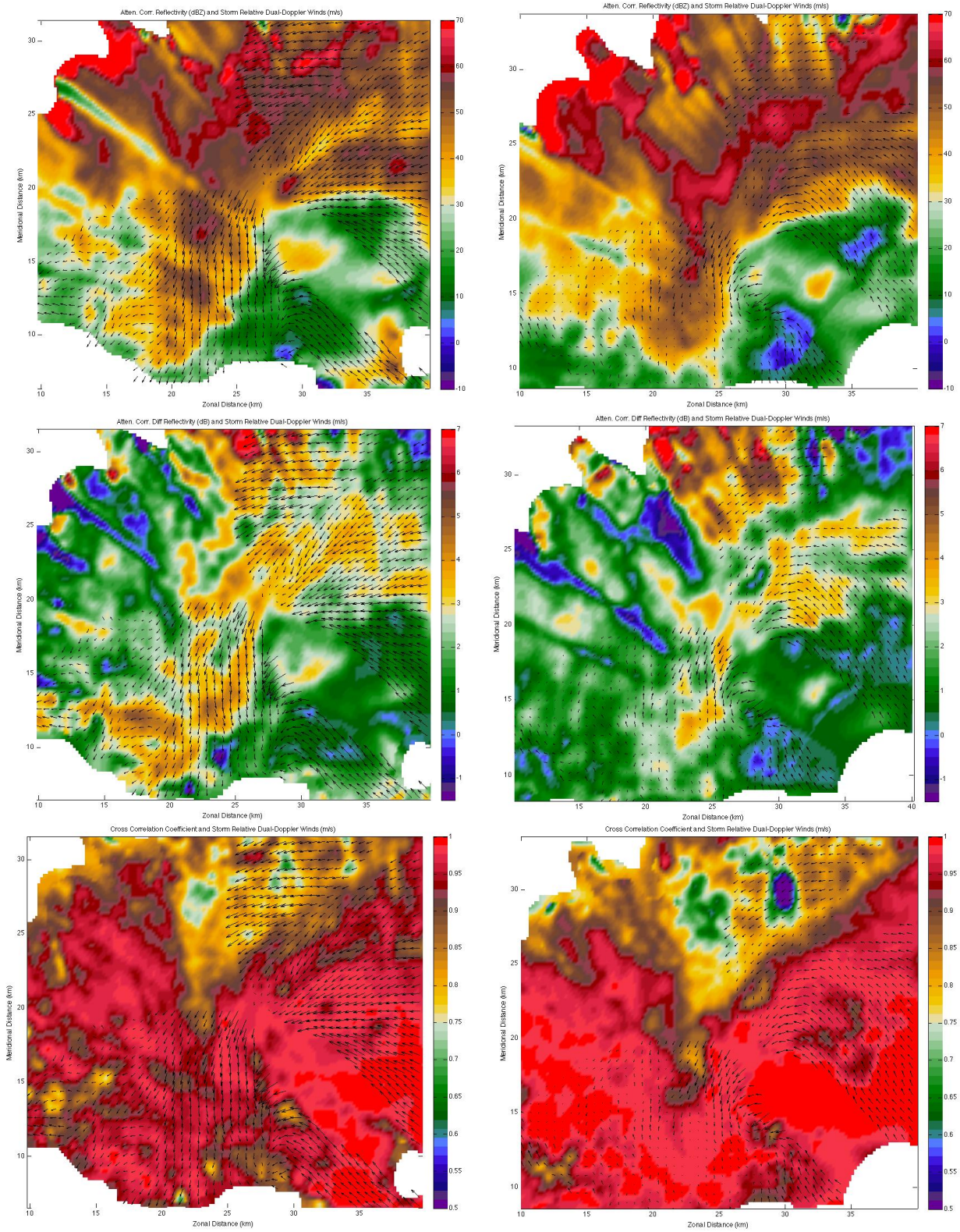


Figure 3. Dual-Doppler analysis from 0116 Z – 0118 Z volume scan. The left column shows data from 600m above radar level (ARL) and the right column shows data from 1800m ARL. The dual-Doppler wind vector field is overlaid with reflectivity (top), differential reflectivity (Zdr; middle) and cross correlation coefficient (R_{hv}; bottom) from NOXP

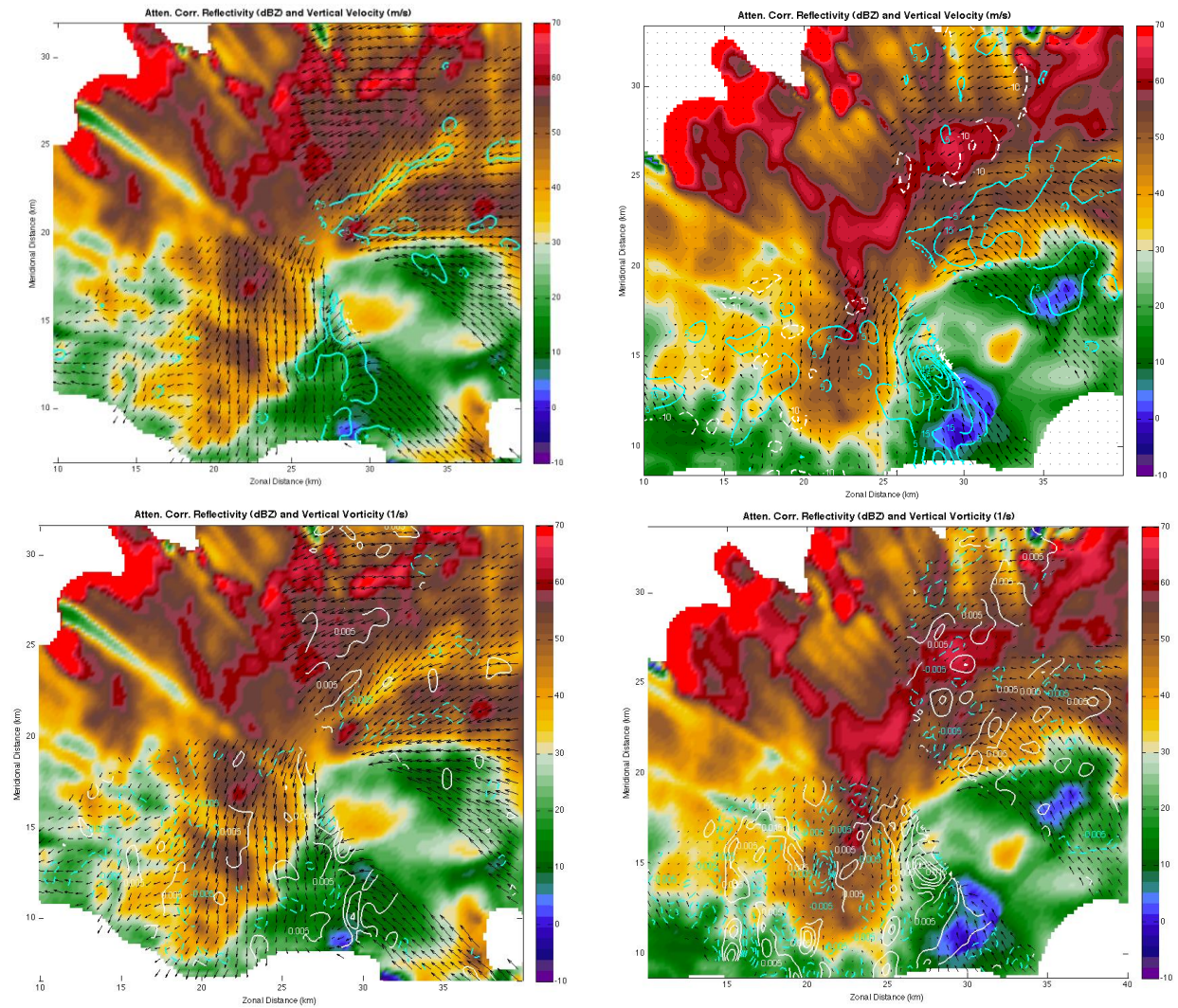


Figure 4. Dual-Doppler wind synthesis vector fields with reflectivity from NOXP at 600m ARL (left) and 1800m ARL (right). Contours of vertical velocity are overlaid (top) and vertical vorticity (bottom). Positive vertical velocity values are in cyan and negative vertical velocity values are in white, while positive vertical vorticity values are in white and negative values in cyan.

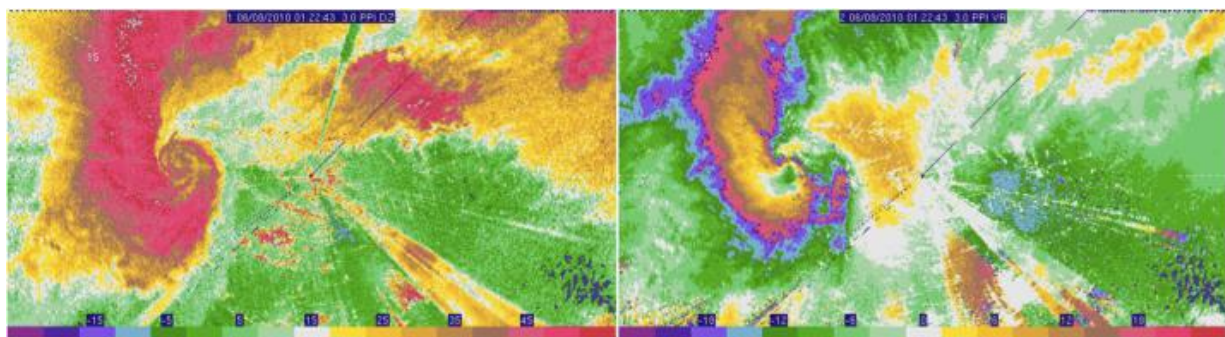


Figure 5. Unedited NOXP radar data at ~0123 Z on June 8, 2010 at 3° elevation showing a low-level hook echo, mesocyclone, tornadic vortex signature (TVS) and strong rear-flank gust front winds; reflectivity (left), radial velocity (right). Image from SOLO II.